Effect of Aging Condition on Semisolid Cast 2024 Aluminum Alloy

Wisutmethangoon S., Pannaray S., Plookphol T., Wannasin J.

Abstract—2024 Aluminum alloy was squeezed cast by the Gas Induced Semi Solid (GISS) process. Effect of artificial aging on microstructure and mechanical properties of this alloy was studied in the present work. The solutionized specimens were aged hardened at temperatures of 175°C, 200°C, and 225°C under various time durations. The highest hardness of about 77.7 HRE was attained from specimen aged at the temperature of 175°C for 36h. Upon investigation the microstructure by using transmission electron microscopy (TEM), the S' phase was mainly attributed to the strengthening effect in the aged alloy. The apparent activation energy for precipitation hardening of the alloy was calculated as 133,805 J/mol.

Keywords—2024 aluminum alloy, Gas induced semi solid, T6 heat treatment, Aged hardening, Transmission electron microscopy.

I. INTRODUCTION

2024 Aluminum (Al) alloy is one of Al-Cu-Mg aged hardenable alloys which are well known for their low weight to strength ratio, good fracture toughness, excellent fatigue properties, and good damage tolerance [1]. Conventionally, 2024 Al alloy was mainly used in the wrought form. However, because of the high cost of a wrought process, gas induced semi solid process (GISS) technology [2] has been applied to the squeeze-casting of 2024 Al alloy.

Further improvement in mechanical properties of 2024 Al alloy can be achieved by T6 heat treatment process which consists of three mainly steps: solution heat treatment, quenching and artificial aging. After quenching and aging at lower temperature, solid solution in the matrix would thus become supersaturated. Precipitation from supersaturated solid solution (SSS) was expected during aging in the temperature range of 160–260°C [3].

There are several precipitation sequences for Al-Cu-Mg alloys have been proposed. One of them was stated by Ringer et al. [4]-[6] and Khan et al. [7]:

$$\alpha_{SSS} \rightarrow \text{Cu:Mg co-clusters/GPB zones} \rightarrow S' / S$$
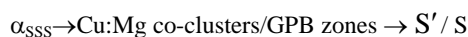
where α_{SSS} is the supersaturated solid solution, GPB is the Guinier Preston Bagaryatsky zones, S' is the intermediate phase, and S is the Al_2CuMg equilibrium phase. Whilst Wang

S. Wisutmethangoon is with the Mechanical Engineering Department, Prince of Songkla University, Hat Yai, Songkhla 90112 Thailand (phone: 66-82-9629966; fax: 66-74-287195; e-mail: sirikul@me.psu.ac.th).

S. Pannaray, T. Plookphol, and J. Wannasinare with the Mining and Materials Engineering Department, Prince of Songkla University, Hat Yai, Songkhla 90112 Thailand.

et al. [3] confirmed no existence of GPB zones but showing the evidence of S'' intermediate phase as proposed:

$$\alpha_{SSS} \rightarrow \text{Cu:Mg co-clusters} \rightarrow S'' \rightarrow S' / S$$
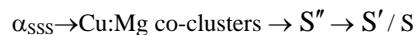
Two distinct stages of precipitation hardening in Al-Cu-Mg alloys have been clarified. The initial stage was attributed to the strengthening by Cu:Mg co-clusters or GPB zones while the latter hardening stage was caused from S' or S phase [3]. Ringer et al. [4]-[6] suggested different hardening mechanism in the second stage. He proposed that the second stage of hardening was due to the formation GPB zones, and overaging occurred as the GPB zones were gradually replaced by the formation and growth of S phase. It is of interest in the present study to determine the proper conditions for solution treatment and aging treatment of GISS processed 2024 Al alloy which provide the desirable mechanical properties. The study of precipitation hardening mechanism is also an attempt in this work.

II. EXPERIMENTAL METHODS

Commercial wrought alloy 2024 was used for rheocasting with GISS technique. Gas bubble was introduced to molten alloy at a temperature of 648°C for 10s and held it for 15s before squeeze-casting with a pressure of about 80 MPa into a bar with the size of 10cm x 10cm x 1.5cm. The as cast specimen was solutionized at 480°C for 14h and followed by quenching in water at room temperature of 25 °C. Artificial aging at temperatures of 175°C, 200°C, and 225°C for various time conditions was then performed in order to study the influence of aging treatment on microstructure and mechanical properties of the alloy.

For microstructure observation on TEM, specimen was machined to a 3mm diameter rod before slicing into 0.8mm thick discs with a Minitom low-speed cut-off machine. Both sides of the discs were ground and polished to about 60μm thickness using 1,200 grit silicon carbide paper and 5μm micro-polishing alumina powder. Discs were further electropolished on a Tenupol-3, Struers polishing machine using a solution of 20% HNO_3 and 80% methanol at a temperature range of -20C° to -30C°. A JEM-2010 JEOL transmission electron microscope, operated at 200 kV, was used to characterize the microstructures of aged specimens. After grinding and polishing specimens by a normal metallographic procedure, hardness of specimens was measured by using Rockwell scale B (HRB).

III. RESULTS AND DISCUSSION

Fig. 1 shows the variations of hardness as a function of logarithmic aging time at different holding temperatures of semi-solid cast 2024 Al alloy produced by GISS technique. From this figure, average peak hardness values were measured to be about 77.7, 73.6, and 75.4 HRB, for aging temperatures of 175°C, 200°C, and 225°C, respectively. Time required for achieving these peak hardnesses was about 36h, 6h, and 1h, respectively, exhibiting a shorter aging time with increasing aging temperature. This is due to higher diffusion rate and hence faster precipitation at higher temperature. The optimum aging time at each aging temperature in the present study were in good agreement with those reported by Khan et al. [8] although 2024 Al alloy was heat treated with different process. In his study of 2024-T351 Al alloys, the optimum aging time at aging temperatures of 170°C, 190°C, 200°C and 220°C was about 30h, 9h, 4h, and 1h, respectively. Shih et al. [1] also reported similar results in aging commercial 2024 Al alloy at 170°C, 190°C, and 240°C in which the peak hardnesses values of about 78 HRB was attained at aging times of 48h, 12h, and 0.25h, respectively. Furthermore, it was revealed from his work that about 50% of the total hardness increase (peak hardness minus SHT hardness) was observed within the first 30sec of aging. This is in good agreement with the present study in that an increase in hardness of about 50% of the total hardening occurred after the first 15min of aging at all three temperatures as illustrated in Fig. 1. Ringer et al. [4]-[6] also noticed a rapid hardening reaction (about 60% of the total hardness increment) within seconds of aging owing to the interaction between Cu:Mg co-clusters and dislocations in the Al-1.1Cu-1.7Mg-T6 alloy. However, no plateau stage after the rapid hardening was observed in this work as was reported by Ringer et al. Only a gradual increase in hardness was evidenced in Fig. 1 when aging longer than 15min at temperatures of 175°C and 200°C and the second stage of hardening was started at the aging times of 12h and 45min, respectively. On the other hand, the second stage of hardening in the specimen aged at 225°C initiated promptly after 15min of aging showing no evidence of gradual hardness increment as depicted in Fig. 1.

Precipitation hardening was studied by TEM observation on specimens aged at 225°C for 15min, 1h, and 12h. Fig. 2 (a) shows the microstructure of the specimen aged for 15 min at 225°C exhibiting high contrast of defects but no precipitate can be resolved. Thus, this partly implied that the hardening phases at the first stage of hardening are likely to be Cu:Mg co-clusters or GPB zones. Moreover, neither formation of S'' nor S' (S) phases were found at this onset of second-stage hardening which was similar to those reported by many authors [4]-[7].With increasing aging time to 1 h, dense and uniformly distributed lath-shaped S' (S) phase was evidenced in Fig. 2 (b). The length of S' (S) lath was measured to be about 300-500nm which is in agreement with 300nm long of S

phase reported by Stoltz et al. [9]. By prolonging aging time to 12h, the S'(S) phase became longer (about 0.8-1µm) and slightly thicker as shown in Fig. 2 (c). According to Shih et al. [1], the lengthening direction of the S' (S) precipitate occurred in the <100> $_{Al}$ direction while the thickening of the S'(S) precipitate was in <011>$_{Al}$ direction by coalescing each other into wide plates and also thickening by the ledge mechanism.

Thus, as of microstructure observation, the following precipitation sequence of the T6-SSM-cast 2024 Al alloy by GISS technique has been proposed:

$$\alpha_{SSS} \rightarrow Cu{:}Mg\ co{-}clusters/GPB\ zones \rightarrow S' / S$$

TEM observation and mechanical properties can be correlated as follows. The rapid hardening effect at the early stage of this alloy was mainly attributed to the Cu:Mg co-clusters. After early rapid hardening, a gradual increase in hardness of specimens aged at 175°C and 200°C was likely to be due to the formation GPB zones although no clear evidence was existed. A specimen aged at 175°C-12h seemed to have a denser GPB zones than that aged at 200°C-45min since a higher hardness was measured from the former specimen. While specimen aged at 225°C was likely to contain none or the lowest amount of GPB zones due to the absence of the slow-increased hardness region. The sudden increase in the second-stage hardening observed in the 225°C aged specimen was derived from the abrupt formation of S'(S) phase by heterogeneous nucleation and growth at both on dislocations and in the matrix away from dislocations [7] since S'(S) phase was the only phase detected at the peak aged specimen as illustrated in Fig. 2 (c). This phase was therefore mainly attributed to the rise in hardness in the second stage of hardening which is in good agreement with the report by Ringer et al. [4]-[6]. It can be deduced from Fig. 1 that the value of hardness increase in the second-stage hardening was highest for specimen aged at 225°C (about 15 HRB) while the specimen aged at 175°C showed the lowest hardness increase (about 8 HRB). This was expected since solid solutions utilized during GPB zones formation in the early stage of aging in the 175°C aged specimens was highest led to the lowest amount of solid solution remained to form S'(S) phase formation at the second-stage hardening. Further aging to the overaged condition results in the drop of hardness owing to the lengthening and coarsening of the equilibrium S phase is shown in Fig. 2 (c) as well as the dissolution of GPB zones.
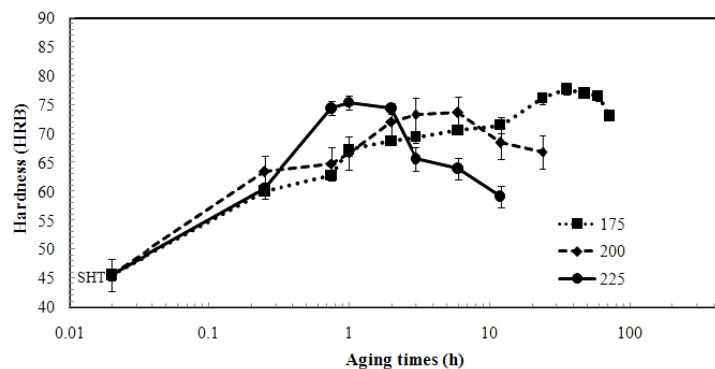
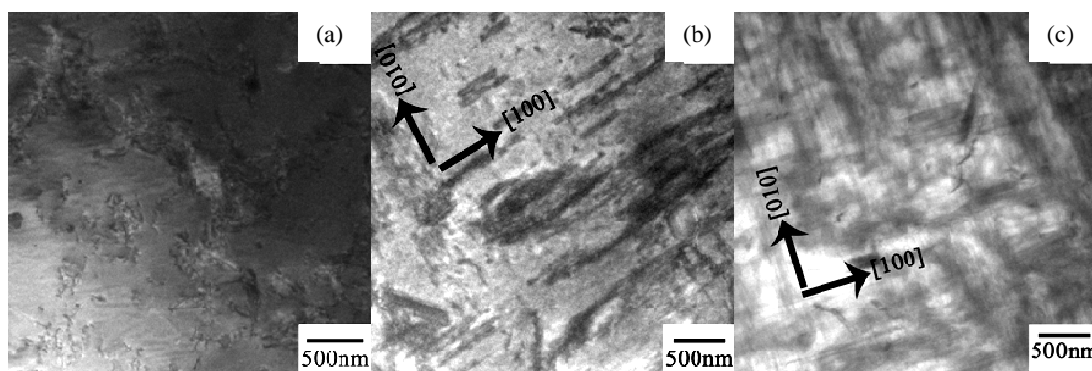Fig. 1 Hardness vs. aging times of the 2024 Al alloy aging at 175°C, 200°C, and 225°C

Fig. 2TEM micrographs and SAD patterns at <100>$_{Al}$ beam direction of the specimens aged at 225 °C for various times of: (a) 15min (underaging), (b) 1h (peak aging), and (c) 12h (overaging), respectively

According to the kinetics of precipitation, one can predict the aging time by deriving apparent activation energy for the precipitation process from an Arrhenius-type equation [10]:

$$t_{T6} = C \exp(Q/RT) \qquad (1)$$

where t_{T6} is the peak hardness time (in seconds), C is the pre-exponential factor, R is the universal gas constant (8.314 J/mol·K), T is the aging temperature (in Kelvin), and Q is apparent activation energy (in J/mol).

By plotting natural logarithmic peak aging time (ln t_{T6}) versus reciprocal aging temperature (1/T) as shown in Fig. 3, the activation energy for precipitation in the GISS processed 2024 Al alloy was calculated to be 133.8 kJ/mol. This activation energy value is similar to that reported in literatures for the formation of S' phase in Al-1.53Cu-0.79Mg (129.9 kJ/mol) [11] while a higher activation energy for S phase formation in 2024-T351 Al alloy has been reported by Khan et al. [7] to be about 133 ± 6 kJ/mol. It is noted that these reported activation energies were close to the diffusion energy of Cu and Mg in Al. Thus, the precipitation sequence of S' (S) phase was controlled by the diffusion of Cu and Mg in the Al matrix. The slight difference in activation energy was due to the differences in the as-received microstructure, chemical composition, heat treatment process, as well as type of precipitation sequence. In this study, the activation energy was

evaluated from the peak aged time at the aging temperatures of 175°C, 200°C, and 225°C. According to the precipitation transformation during the initial aging through the peak aging, one could be able to predict time to reach the optimum hardness in the GISS processed 2024-T6 Al alloy by substituting apparent activation energy of 133.8 kJ/mol into (1).
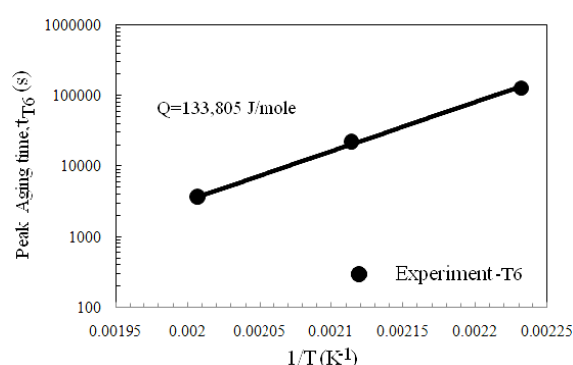

Fig. 3 Arrhenius-type plot between the peak hardness time (t_{T6}) and the reciprocal of aging temperature (1/T) of 2024 Al alloy produced by GISS technique

IV. CONCLUSIONS

1. Precipitation sequence of the T6-SSM-cast 2024 Al alloy by GISS technique has been proposed as:

$$\alpha_{SSS} \rightarrow \text{Cu:Mg co-clusters/GPB zones} \rightarrow S'/S$$

2. Cu:Mg co-clusters formed at the early stage of aging and were ascribed for the sudden increase in hardness at the first stage of hardening. Further aging results in the gradual rise of hardness owing to the formation of GPB zones.

3. Lath-shaped $S'(S)$ precipitate rapidly formed after the onset of the second stage of hardening, and was mainly contributed to the hardening effect at this stage.

4. Peak hardness value of 77.7, 73.6, and 75.4 HRB was attained when aging for 36 h, 6 h, and 1 h at aging temperatures of 175℃, 200°C, and 225°C, respectively.

5. Prolonged aging to the overaged condition results in the lengthening of the $S'(S)$ phase from about 300-500 nm long to about 0.8-1 µm long.

6. Apparent activation energy (Q) for precipitate sequence to the peak aging condition was 133,805 J/mol.

REFERENCES

[1] H.C. Shih, N.J. Ho, J.C Huang, Metall. Mater. Trans. A 27 (1996) 2479-2494.
[2] J. Wannasin, S. Janudom, T. Rattanochaikul, R. Canyook, R. Burapa, T. Chucheep, S.Thanabumrungkul, T. Nonferr. Metal. Soc. 20 (2010) 1010-1015.
[3] S.C. Wang, M.J. Starink, N. Gao, Scripta Mater. 54 (2006) 287-291.
[4] S. Ringer, K. Hono, T. Sakurai, I.J. Polmear, Scripta Mater. 36 (1997) 517-521.
[5] S. Ringer, T. Sakurai, I.J. Polmear, Acta Mater. 45 (1997) 3731-3744.
[6] S.P. Ringer, K. Hono, Mater. Charact. 44 (2000) 101-131.
[7] I.N. Khan, M.J. Starink and J.L. Yan,Mater. Sci. Eng., A 472(2008) 66-74.
[8] A.M. Zahra, C.Y. Zahra, W. Lacom, K. Spiradek, Proc. Int. Conf. on Light Metals, Amsterdam, 20-22 June 1990, ed. T. Khan and G. Effenberg (1990) 633.
[9] S.C. Wang, M.J. Starink, Int. Mater. Rev. 50 (2005) 193-215.
[10] H. Möller, G. Govender, W.E. Stumpf, The Open Mater. Sci. J. 2 (2008) 6-10.
[11] A.K. Jena, A.K. Gupta, M.C. Chaturvedi, Acta Metall. 37 (1989) 885-895.